Photoionization spectral hole burning and its erasure in $Li_2Ge_7O_{15}:Cr^{3+}$: Effects of site-dependent energy-level shifts within the band gap

S. A. Basun, S. P. Feofilov, and A. A. Kaplyanskii
A.F. Ioffe Physico-Technical Institute, Academy of Sciences of Russia, 194021 St. Petersburg, Russia

U. Happek, J. Choi, K. W. Jang,* and R. S. Meltzer
Department of Physics and Astronomy, University of Georgia, Athens, Georgia 30602
(Received 27 May 1999; revised manuscript received 8 December 1999)

We report on investigations of the dependence of ionization spectral hole burning efficiencies on the location of impurity ion energy levels relative to both the host valence band and the conduction band. An ideal system is Cr-doped $Li_2Ge_7O_{15}$, where the Cr^{3+} ions occupy three distinct noncentrosymmetric Ge^{4+} sites, which differ from one another by the location of their charge-compensating ions. Most important for our investigation is the large ($\sim$eV) and site-specific shift of the Cr^{3+} energy levels relative to the host valence and conduction bands. As a result, only one of the three sites shows persistent spectral hole burning. It is shown that this result can be understood from an analysis of the differences of the energy-level locations of the ground and excited states of the three Cr^{3+} centers relative to the host bands. Two of the centers have their energy levels sufficiently close to the host conduction band such that two-step ionization, and thus persistent spectral hole burning, can occur. However, for one of the centers the ground state lies so close to the valence band that an erasure process involving promotion of an electron from the valence band to the ionized center leads to the restoration of the initial charge state. This erasure process, clearly demonstrated in this paper, has to be considered when evaluating the hole burning potential of doped insulators, especially those with relatively narrow band gaps.

I. INTRODUCTION

If impurity ions are stable in more than one valence state, photoionization can lead to persistent spectral hole burning (PSHB).[1] This effect reveals important fundamental information on the homogeneous linewidth of electronic transitions of impurity ions, is a tool to investigate dynamical processes in ordered and disordered solids, and has the potential of providing a mechanism for high-density data storage and optical processing.[1] Photoionization occurs under monochromatic irradiation resonant with a subset of ions within the inhomogeneously broadened zero-phonon line and produces a stable spectral hole by converting some of the resonant ions to the oxidized valence state. A number of interesting questions are connected with the mechanism of the photoionization: the ionization process, the nature of the traps involved, and the processes by which the charge transport occurs. Here, the process of photoionization spectral hole burning (chemical hole burning) occurs in two steps. In the first step, resonant absorption of the monochromatic light excites the ion from its ground state to its excited metastable state. In the second step, photoionization of the ion takes place by promoting the impurity electron from the metastable state to the conduction band via absorption of a second photon, provided either by the monochromatic source used to excite the ion to the metastable state or a secondary source. A central issue in understanding the processes involved in the photoionization is the location of the ground and excited levels of the dopant ion relative to the insulator conduction band: the photon energies of the light sources used have to be large enough to bridge the two energy gaps involved in the ionization process. While focusing on the ionization (donor) process, a second, equally important process has been generally overlooked: charge-transfer (acceptor) processes that promote an electron from the valence band to the impurity ionized in the hole-burning process. Since charge-transfer processes have a large cross section, they can be more efficient than two-step ionization processes. These may strongly quench the hole-burning process when the ground state of the impurity ion is sufficiently close to the valence band. In this paper we demonstrate the importance of this process.

The importance of the role of the impurity ground-state location relative to the host valence band can be demonstrated in a system where a single probe ion occupies different sites. These sites should differ in the location of the impurity energy levels with respect to the host bands, while retaining the energy gap between the impurity ground and first excited metastable state. This kind of system has been realized in Cr-doped lithium heptagermanate crystals, $Li_2Ge_7O_{15}$, (LGO) codoped with Mg, where the Cr^{3+} ions occupy three distinct sites. These Cr^{3+} centers differ from one another by the location of their charge-compensating ions resulting in a large and site-specific shift of the Cr^{3+} energy levels relative to the host valence and conduction bands.[2] These shifts are caused by a combination of the local Coulomb field resulting from the different types and locations of the charge-compensating ions and the lack of inversion symmetry of the sites, producing large ($\sim$eV) relative linear Stark shifts. Furthermore, the optical properties of LGO:Cr^{3+},Mg have been studied previously,[2] and a photocurrent under resonant excitation in the R lines ($^4A_2 \Rightarrow {}^2E$ transition) for two of the three Cr^{3+} centers was observed. This provides direct evidence for two-step photoionization of these two Cr^{3+} centers via the intermediate ^2E state, allowing two-photon hole burning.

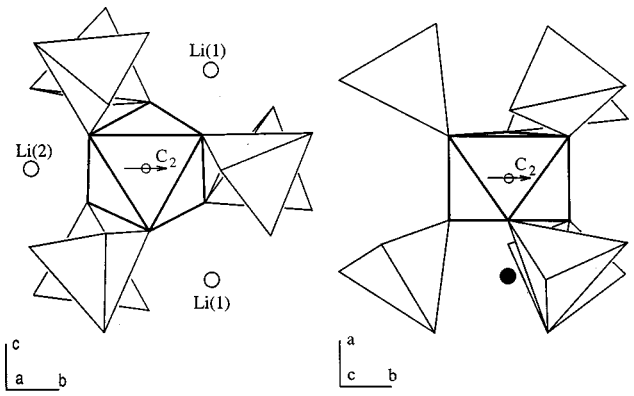

FIG. 1. Fragments of $Li_2Ge_7O_{15}$ paraphase lattice projected on the ''*bc*'' plane (left) and the ''*ab*'' plane (right) after (Refs. 4 and 5). An octahedron of GeO_6 with its surrounding tetrahedra of GeO_4 is shown. Small open circles, position of octahedral Ge^{4+} substituted by Cr^{3+} ion. Large circles, Li^+ ion positions: regular Li(1) and Li(2) (open circles) and nonstoichiometric interstitial (solid circle). Arrows indicate the directions of the permanent dipole moments of Cr^{3+}.

II. SAMPLE PREPARATION AND CHARACTERIZATION

Single crystals of LGO doped only with Cr (LGO: 0.02% Cr), and codoped with Mg (LGO: 0.02% Cr, 0.02% Mg), were studied. The crystals were grown by the Czochralskii method in Sevastyanov's group of the Institute for Crystallography, Moscow.

Chromium-doped LGO crystals display narrow zero-phonon *R* lines of the ''Cr^{3+}-Li^+'' center corresponding to transitions between ground ($^4A_2$) and excited (^2E) states of Cr^{3+} ions in an octahedral coordination. Double-doping LGO crystals with Cr and Mg leads to two more Cr^{3+} centers. These centers differ in their type and in the location of the adjacent charged defect providing local compensation to the excess negative charge of the Cr^{3+} ion which substitutes for Ge^{4+} in the GeO_6 octahedron[2] (see Fig. 1). For the Cr^{3+}-Li^+ center, the charge compensation is provided by an interstitial Li^+ ion shifted along the *a* axis relative to $Cr^{3+}(Ge^{4+})$. For two types of Mg-compensated centers, the charge compensation is provided by Mg^{2+} substitution either on a Li(1) site [Cr^{3+}-Mg^{2+}(1) center] or on a Li(2) site located on the twofold C_2 symmetry axis passing through the center of the GeO_6 octahedron [Cr^{3+}-Mg^{2+}(2) center]—see Fig. 1. Spectroscopically, the different sites are reflected in a shift of the *R* lines. The *R*-line luminescence spectra at 77 K [well below the ferroelectric transition temperature of 280 K (Ref. 3)] of both the Cr^{3+} and Cr^{3+}, Mg^{2+} samples are shown in Fig. 2. The assignments of the different transitions have been previously reported.[2] The *R* lines associated with the Cr^{3+}-Li^+ center occur in both the Cr^{3+} and doubly doped Cr^{3+},Mg^{2+} samples. In the ferroelectric phase, two sets of *R* lines (*R* and *R'*) are observed for this site. At helium temperature the R_1 and R_1' lines occur at 695.4 and 696.1 nm, respectively. In the doubly doped Cr^{3+},Mg^{2+} sample, two additional sets of *R* lines are observed. The first Mg-compensated, triclinic, center, Cr^{3+}-Mg^{2+}(1), displays $^tR_1$,$^tR_1'$ lines at 697.3 and 697.6 nm. The second Mg-compensated, monoclinic, center, Cr^{3+}-Mg^{2+}(2), shows only a single $^mR_1$ line at 694.0 nm. All wavelengths are given for

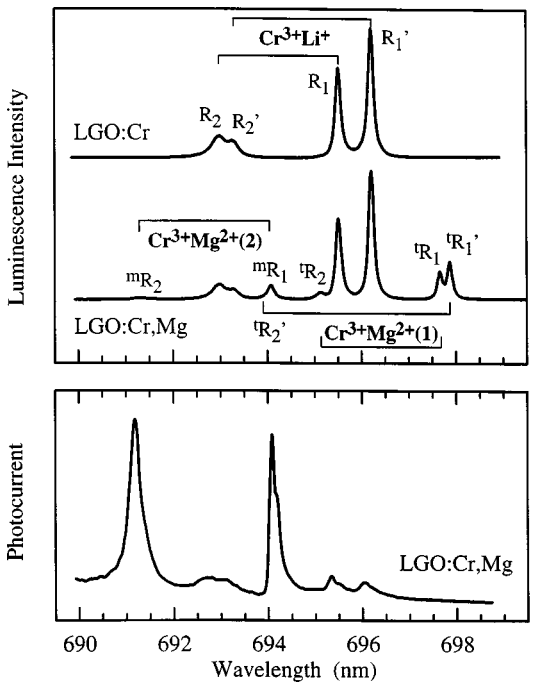

FIG. 2. Luminescence spectra at $T=78$ K (top) and ''resonant'' photocurrent excitation spectrum at $T=2$ K (bottom).

$T=2$ K, the temperature relevant for the hole-burning experiments presented in this paper. We would like to note at this point already that the shift of the *R* lines is relatively large, indicating strong internal electric fields due to the Li and Mg charge-compensating ions. Two-step photoionization observed in the photoconductive response under resonant excitation of the Cr^{3+}-Mg^{2+}(2) and Cr^{3+}-Li^+ centers ($^mR_1$, $^mR_2$, and R_1, R_1', R_2, R_2') is shown in Fig. 2, indicating the potential of photochemical hole burning of two of the three sites.

III. SPECTRAL HOLE BURNING

Spectral hole burning was studied on the *R* lines [$^4A_2 \rightarrow E(^2E)$ transitions] from the ground $^4A_2$ state to the lowest sublevel of the metastable ^2E doublet of Cr^{3+} centers of the three different centers described above.

The burning and detection of persistent spectral holes within the *R*-line contours were carried out with a Coherent CR 899 ring dye laser using the dye DCM Special producing a laser linewidth of 0.5 MHz. Samples were immersed in liquid helium ($T=2$ K) inside an optical cryostat. Spectral holes were observed by scanning the laser frequency while simultaneously observing the fluorescence in the phonon sideband emission of the $^2E \rightarrow {}^4A_2$ transition with a photomultiplier (PMT). The detection was performed at powers well below those used for hole burning by decreasing the laser power by three orders of magnitude using neutral density glass filters. We note that scanning did not cause any erasure of the burnt holes. The detection spectral region in the phonon sidebands was isolated from the excitation light with an interference band-pass filter (710 nm, 10 nm FWHM) in front of the PMT. The output of the PMT was recorded with a digital storage scope, using a ratioing technique to normalize the excitation spectrum to the laser inten-

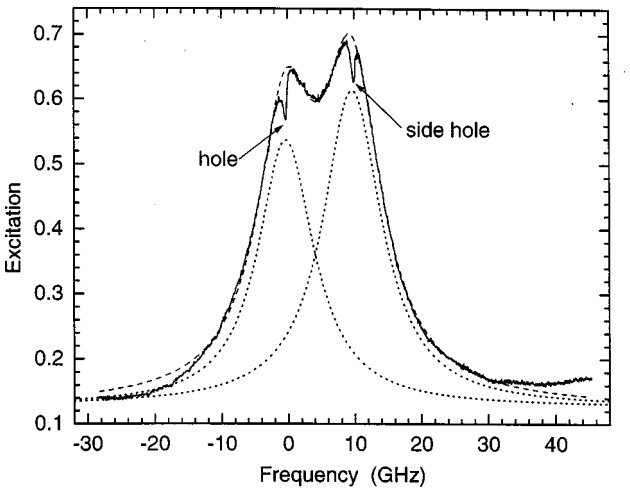

FIG. 3. ${}^mR_1$ line shape at a temperature $T=2$ K. Solid line: luminescence excitation spectrum after burning at 694.0 nm. Dashed and dotted lines: two Lorentzian fit to the ${}^mR_1$ line shape before burning and its separate components, respectively.

sity and to compensate for fluctuations of the laser power. In this way it was possible to perform a step-by-step scan over the whole zero-phonon line, although the R_1 lines in LGO:Cr^{3+} are several times broader than the laser scan range (20 GHz).

The luminescence excitation spectrum after burning a spectral hole at 694.0 nm is shown in Fig. 3. The doublet character of the ${}^mR_1$ line shape results from the ${}^4A_2$ ground-state splitting. The value of the splitting is obtained by fitting the observed spectrum to two Lorentzians of identical widths using a variable splitting. The magnitude of the splitting, 10.0 ± 0.2 GHz, is similar to that seen for Cr^{3+} in other hosts.[6–8] Very similar splittings were also found for the other R_1 lines of LGO:Cr, Mg (R_1, R_1', ${}^tR_1$, and ${}^tR_1'$). In addition to the hole observed at the laser frequency, a sidehole, shifted to higher frequency by 10.1 ± 0.1 GHz, is seen in Fig. 3. It occurs because the first site-selective step in the photoionization process results from excitation of the Cr^{3+} from its upper ground-state component (the laser was tuned to the low-frequency part of the absorption doublet). Since the photoionization process oxidizes the Cr^{3+} ions resonant with the laser, their total contribution to the absorption spectrum is removed. Hence a reduced absorption is also seen at frequencies resonant with transitions from the lower ground-state component. Deep persistent holes were observed at all frequencies within the inhomogeneously broadened ${}^mR_1$ doublet. The sidehole is observed shifted either to lower or higher frequencies than the main hole by 10.1 ± 0.1 GHz depending on where the laser was tuned within the doublet structure. Within experimental error, the splitting is always the same as the splitting of the doublet in the excitation spectrum.

To study the depth and width of spectral holes as a function of burning time, a spectral hole was burnt at a fixed wavelength, 694.0 nm, with a weak incident power density of 80 mW cm^{-2}. The depth of the hole rises with increasing burning time and reaches a value of more than 20% (Fig. 4). The width of the hole is about 300 MHz and broadens only slightly with an increase in the hole depth (Fig. 4, inset). It is seen from Fig. 4 that even a hole depth as large as 20% is

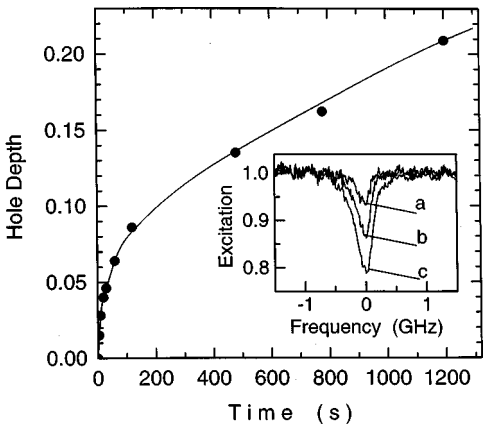

FIG. 4. Hole depth vs period of burning at 694.0 nm with 80 mW cm^{-2} at a temperature of $T=2$ K. Inset: spectral hole profiles after 60, 480, and 1200 s of burning (*a*, *b*, and *c*, respectively).

still far from the saturated value. With an increase of incident power density, the rate of burning increases rapidly; with 1 W cm^{-2} it takes only a few seconds to burn a hole with a depth of ~10%.

The absence of the hole burning on the Cr^{3+}-Mg^{2+}(1) center is consistent with our findings that a two-step process does not bridge the gap between the Cr^{3+} ground state and the conduction band, as is evident from the lack of an observable photocurrent under resonant excitation (see Fig. 2). However, it is surprising that the Cr^{3+}-Li^+ center does not exhibit hole burning, although two-step resonant excitation leads to photoionization. It is important to note that on the zero phonon R_1 lines of the Cr^{3+}-Mg^{2+}(1) and Cr^{3+}-Li^+ centers, no hole burning was observed even with much higher incident power densities (up to 100 W cm^{-2}, and burning periods of up to several tens of minutes) than those used for the Cr^{3+}-Mg^{2+}(2) center.

IV. DETERMINATION OF THE Cr^{3+} ENERGY LEVELS WITH RESPECT TO THE HOST BANDS

To tie these hole-burning results to the location of the Cr^{3+} energy levels with respect to the host conduction and valence bands, photocurrent excitation spectroscopy (photoconductivity) was performed.

For the photoconductivity experiments, the samples are mounted on the coldfinger of a temperature variable cryostat, pressed between two nickel meshes that serve as transparent electrodes. Photocurrents are excited by a 300 W Xe arc lamp spectrally filtered by an f/2 double monochromator (McPherson) and measured with a Keithley 6517 electrometer. To utilize the high sensitivity of the electrometer, additional features of the setup include electrical shielding and high mechanical stability of the sample mount, resulting in detectable photocurrents of less than 10^{-15} A. Typically, a field of up to 10 kV/cm is applied across the sample, which results in stationary photocurrents on the order of 10^{-15}–10^{-12} A.

As a general rule, photoconductivity data can be properly interpreted only in conjunction with complementary absorption, emission, and excitation spectra. Emission and absorption data were taken from previous publications.[2] Additional

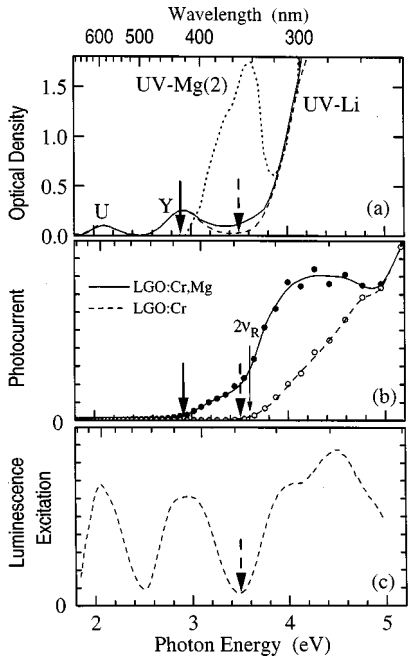

FIG. 5. (a) Absorption, (b) one-step photocurrent excitation spectra of $Li_2Ge_7O_{15}$:Cr and $Li_2Ge_7O_{15}$:Cr,Mg crystals, and (c) photoluminescence excitation spectrum of $Li_2Ge_7O_{15}$:Cr monitored at 700 nm. All spectra taken at $T=300$ K. The excitation spectra (b) and (c) are normalized to the incident photon flux. The locations of the long-wavelength thresholds of the photocurrent excitation and uv absorption bands of the Cr^{3+}-Mg^{2+}(2) centers and Cr^{3+}-Li^+ centers are indicated by thick solid arrows and thick dashed arrows, respectively. Thin arrow (b): doubled *R*-photon frequency.

photoexcitation spectra were recorded using a SPEX fluorometer.

The absorption spectrum of the singly doped sample exhibits, in addition to the intra-ion Cr^{3+} absorption bands, $U(^4A_2 \rightarrow {}^4T_1)$ and $Y(^4A_2 \rightarrow {}^4T_2)$, a strong uv absorption band with a threshold at about 350 nm (3.5 eV), labeled uv-Li in Fig. 5(a). This has been ascribed to the absorption of Cr^{3+}-Li^+ centers caused by one-photon donor-type ionization of the Cr^{3+} ion from the $^4A_2$ ground state.[2] In the double-doped sample, an additional uv absorption band can be observed. Since this band overlaps the *Y* and uv-Li bands, we have plotted in Fig. 5(a) this band [labeled uv-Mg(2)] as the difference in the absorption of the two samples, multiplied by the ratio of the $Cr^{3+}Mg^{2+}$(2) to Cr^{3+}-Li^+ concentration. The concentration ratio was estimated by comparing the fluorescence intensities under excitation into the *Y* band. The normalized presentation reveals an absorption onset of the uv-Mg(2) band at 3.0 eV, which has been assigned to the ionization of Cr^{3+} on the Cr^{3+}-Mg^{2+}(2) center.[2]

A direct confirmation that these uv-Li and uv-Mg(2) absorption thresholds correspond to the energy difference between the $^4A_2$ levels of these centers and the bottom of the conduction band is obtained through the measurement of the long-wavelength threshold of the one-photon photoconductivity spectra. Figure 5(b) shows the one-photon excitation spectra of the stationary conductivity measured on the singly doped Cr^{3+} and the doubly doped Cr^{3+},Mg^{2+} samples. For the single-doped samples, where Cr^{3+}-Li^+ centers dominate, a conductivity threshold is observed at 3.5 eV that matches the onset of the uv-Li absorption band. For the double-doped samples, we find an additional threshold at 430 nm (2.9 eV), an energy that matches the onset of the uv-Mg(2) absorption band. This demonstrates that the uv-Li band and the uv-Mg(2) bands do not reflect intra-ion transitions, but a promotion of an impurity electron to the conduction band. In addition, these results give evidence of a very large shift of the impurity energy levels relative to the conduction band due to different charge compensators. The relative location of the Cr^{3+}-Li^+ and Cr^{3+}-Mg^{2+}(2) energy level shifts with respect to the host conduction band by $3.5-2.9\,\text{eV}=0.6\,\text{eV}$, more than 10% of the host band gap.

The assignment of the uv bands to Cr^{3+} ions is unambiguously obtained from the *R*-line luminescence excitation spectrum [Fig. 5(c)]. The *R*-line luminescence excitation spectrum displays, in addition to the intra-ion *U* and *Y* bands, an additional band whose long-wavelength threshold, 3.5 eV, exactly matches the onsets of the uv-Li band observed in absorption [Fig. 5(a)] and photocurrent excitation spectra [Fig. 5(b)]. Cr^{3+} luminescence is excited via ionization in a series of steps. The mechanism involves photoionization, $Cr^{3+}+h\nu_{\text{exc}} \Rightarrow Cr^{4+}+e(\text{CB})$, i.e., conversion of Cr^{3+} to Cr^{4+} accompanied by generation of a photoelectron in the conduction band, e(CB). At the second phase of the process, recombination of the photoelectron with a Cr^{4+} ion results in the formation of a Cr^{3+} ion in the excited state, ^2E, followed by emission of an *R* photon: $e(\text{CB})+Cr^{4+} \Rightarrow Cr^{3+}(^2E) \Rightarrow Cr^{3+}(^4A_2)+h\nu_R$.

We would like to point out that the uv absorption bands could in principle reflect charge-transfer processes (promoting a valence-band electron to a Cr^{4+} ion). However, in this case the low-energy threshold of the absorption band cannot lead to Cr^{3+} emission, in contradiction to our observations [Fig. 5(c)]. Thus, the coincidence of the onsets of the uv absorption, photoconductivity, and luminescence excitation of the Cr^{3+} emission strongly supports our assignment of the uv bands to donorlike processes.

V. Cr^{3+}-HOST ENERGY-LEVEL DIAGRAM AND BORN-HABER CYCLE

These experimental results lead to a combined host-impurity energy-level diagram for the different Cr^{3+} centers (similar to the approach commonly used for doped semiconductors), shown in Fig. 6, which indicates the locations of the $^4A_2$ and ^2E levels of the Cr^{3+}-Li^+ and Cr^{3+}-Mg^{2+} centers in the band gap. For the Cr^{3+}-Li^+ and Cr^{3+}-Mg^{2+}(2) centers, the photon energy required to induce the first site-selective $^4A_2$-^2E transition exceeds the energy which is necessary for photoionization from the metastable ^2E state. This assignment is supported by the observation[2] of resonant excitation of photocurrent in the *R* lines of both the Cr^{3+}-Li^+ and Cr^{3+}-Mg^{2+}(2) centers (see Fig. 2) which can occur in two steps via the intermediate state, ^2E. The much higher efficiency of resonant two-step photoionization of the Cr^{3+}-Mg^{2+}(2) centers compared to that of the Cr^{3+}-Li^+ centers (Fig. 2) is due to the fact that the doubled *R* photon frequency [marked by a thin arrow $2\nu_R$ in Fig. 5(b)] corresponds to a frequency near the maximum in photoconductivity for Cr^{3+}-Mg^{2+}(2) but to the very weak long-wavelength tail for Cr^{3+}-Li^+ centers. For the Cr^{3+}-Mg^{2+}(1) center we

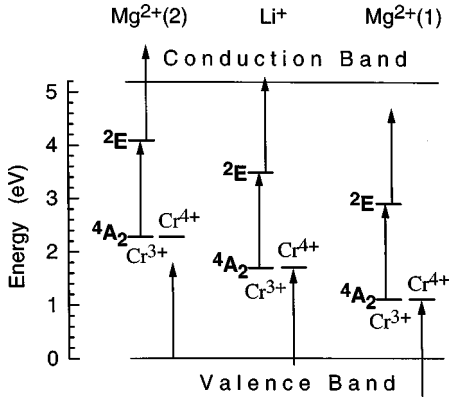

FIG. 6. Energy-level scheme of different Cr^{3+} centers in the band gap of $Li_2Ge_7O_{15}$. Shown are the $^4A_2$ and ^2E levels of Cr^{3+} and the valence and conduction bands.

must assume that the ground-state energy is lower than that of the other two centers, since no ionization is observed (Fig. 2). Evidence for its placement in the energy-level diagram will be presented below.

While the location of the Cr^{3+} ground states with respect to the host conduction band explains why it is possible to burn spectral holes on the $^mR_1$ line of Cr^{3+}-$Mg^{2+}(2)$ centers, it cannot explain the absence of two-step hole burning on the R_1 and R_1' lines of Cr^{3+}-Li^+ centers. As pointed out already, the energy locations of their $^4A_2$, ^2E levels in the band gap of LGO (Fig. 6) allow for the two-step ionization by R_1, R_1' photons. Moreover, the existence of photoionization for these centers has been directly proven by the observation of a photocurrent under resonant excitation into their R_1 lines as shown in Fig. 2. For efficient hole burning traps have to be present in the sample. Since deep persistent spectral holes are observed for the Cr^{3+}-$Mg^{2+}(2)$ centers, the presence of traps is evident, and a lack of traps cannot be an argument for the lack of spectral holes on the R_1, R_1' lines of the Cr^{3+}-Li^+ centers.

In order to explain the absence of holes for the Cr^{3+}-Li^+ center, we have also to consider the location of the ground state of this center with respect to the valence band. The location of the top of the valence band relative to the $^4A_2$ levels can be obtained according to the Born-Haber cycle principle.[9] In accordance with this very general thermodynamic principle, the sum of the threshold energies of donorlike and acceptorlike electron transitions (from the impurity to the conduction band and from the valence band to the *ionized* impurity, respectively) equals the host band gap E_g. For both the Cr^{3+}-Li^+ center and Cr^{3+}-$Mg^{2+}(2)$ center, the donorlike (ionization) thresholds are known (see above). With a host band gap of $E_g = 5.2$ eV (Ref. 10) this allows one to estimate the corresponding acceptorlike thresholds. These thresholds are the energies necessary to promote valence-band electrons to Cr^{4+} ions, thereby converting them to the trivalent state. The resulting locations of the $^4A_2$ levels of Cr^{3+}-Li^+ and Cr^{3+}-$Mg^{2+}(2)$ centers in the band gap of LGO are shown in the lower part of Fig. 6. As seen from Fig. 6, the energy of the acceptorlike transition of the Cr^{3+}-Li^+ center equals 1.7 eV, 0.1 eV less than the *R*-photon energy (1.8 eV and shown by the arrows in Fig. 6). Thus an acceptorlike transition can be induced by the laser radiation (1.8 eV) used to selectively create the hole: electrons are promoted optically from the valence band to the Cr^{4+} previously formed by the two-step photoionization of Cr^{3+}. This effectively restores the initial charge state, Cr^{3+}, for the Cr^{3+}-Li^+ centers, thereby erasing the spectral hole.

The processes of burning and erasure compete with one another in such a way that an observable persistent spectral hole is not formed. The hole burning takes place via a two-step process, with the first step of the ionization process partly forbidden by selection rules. However, the erasure of the burnt hole occurs in a one step acceptorlike process. These charge-transfer processes are known for their large transition matrix element. As a result of the competition, burning of holes is impossible under these conditions. For the Cr^{3+}-$Mg^{2+}(2)$ center, however, which shows efficient hole burning, the minimum energy necessary for a similar acceptorlike transition equals 2.3 eV and the *R* photon (1.8 eV) cannot induce an acceptorlike hole erasure transition.

To summarize, the hole burning efficiency crucially depends on the location of the impurity ion energy levels with respect to the host bands, and LGO:Cr:Mg is an ideal system to study the different scenarios. For the Cr^{3+}-$Mg^{2+}(2)$ center, two-step ionization does occur, and since erasure due to acceptorlike processes is forbidden, efficient hole burning is observed. For the Cr^{3+}-Li^+ center, two-step ionization is also allowed, but the burnt holes are immediately erased via promotion of valence-band electrons to the tetravalent chromium ions, thereby eliminating the holes. Finally, the Cr^{3+}-$Mg^{2+}(1)$ center shows no hole burning due to the large energy difference between the $^4A_2$ ground state and the conduction-band bottom, making ionization spectral hole burning impossible. The erasure of spectral holes in the *R* lines of Cr^{3+} in insulators with a band gap which is not too wide with respect to the Cr^{3+} transitions was discussed earlier[11] regarding experiments on $SrTiO_3$:Cr.[12] In that system the erasure efficiency as a function of frequency[12] showed the same threshold as the acceptorlike charge-transfer process from the valence band to Cr^{4+}, which was identified by means of photo-EPR.[11]

VI. IMPURITY GROUND-STATE SHIFT DUE TO THE STARK EFFECT

These results point to the large Stark shifts observed for the ground-state levels of different Cr^{3+} centers relative to the host bands. While these centers appear to be very similar with respect to intra-ion transitions (the *R*-line energies vary only by 0.5%), the position of the ground states relative to the host bands is strongly influenced by the Stark effect caused by local charge compensation. In LGO:Cr^{3+} this leads to variation of the ground-state energy with respect to the host band gap by more than 10%.

While the Stark shifts can be obtained directly for the Cr^{3+}-Li^+ and the Cr^{3+}-$Mg^{2+}(2)$ centers, the location of the $^4A_2$ level of the Cr^{3+}-$Mg^{2+}(1)$ center in the band gap of LGO could not be found directly. However, using the results on the Cr^{3+}-Li^+ and the Cr^{3+}-$Mg^{2+}(2)$ centers, the position of the Cr^{3+}-$Mg^{2+}(1)$ center can be estimated in an indirect way based on the microstructure of the centers. This estimate is built on the assumption that the relative shift of the *R*-line positions of the different sites is a measure of the local Cou-

lomb field due to the charge-compensating ions and that this field also causes the shift of the $^4A_2$ ground state relative to the host bands. Because the Cr^{3+} ion substituting on the octahedral Ge^{4+} site has no inversion symmetry (point symmetry group C_2), the Cr^{3+} ion possesses a permanent dipole moment directed along the C_2 axis (arrow on C_2 site in Fig. 1). In the different types of Cr^{3+} centers, the charge defects which provide the charge compensation are in different locations with respect to the Cr^{3+} ion and its dipole moment.[2] The projection of the Coulomb field of the charged defect on the permanent dipole moment of Cr^{3+} is zero for Cr^{3+}-Li^+ centers and has the opposite sign for the two types of $Cr^{3+}Mg^{2+}$ centers (see Fig. 1). Therefore, the linear Stark shift of the energy levels (and spectra) of Cr^{3+} in the Cr^{3+}-$Mg^{2+}(1)$ and Cr^{3+}-$Mg^{2+}(2)$ centers should have the opposite sign relative to the position of the levels of the Cr^{3+}-Li^+ centers. This situation is observed experimentally for the *R* lines of $Cr^{3+}Mg^{2+}(1)$ and $Cr^{3+}Mg^{2+}(2)$, which are shifted by a similar amount in opposite directions relative to the *R* lines of Cr^{3+}-Li^+ centers (see Fig. 2). Based on the nearly symmetric location of the Cr^{3+}-$Mg^{2+}(2)$ and Cr^{3+}-$Mg^{2+}(1)$ *R*-line transition energies relative to those of Cr^{3+}-Li^+, we estimate that the linear Stark shifts of the $^4A_2$ ground level of Cr^{3+} with respect to the host band edges in the Cr^{3+}-$Mg^{2+}(1)$ and Cr^{3+}-$Mg^{2+}(2)$ centers are also nearly equal in magnitude but opposite in sign relative to that of the Cr^{3+} ion in the Cr^{3+}-Li^+ center. The shift of the $^4A_2$ ground level of Cr^{3+} in the Cr^{3+}-$Mg^{2+}(2)$ center was determined experimentally from the difference in the one-photon PC thresholds for the Cr^{3+}-Li^+ and Cr^{3+}-$Mg^{2+}(2)$ centers to be 0.6 eV (Fig. 5). Hence we can assume that the $^4A_2$ level of the Cr^{3+}-$Mg^{2+}(1)$ centers is located in the energy gap of LGO $\sim$0.6 eV below the $^4A_2$ level of Cr^{3+}-Li^+, i.e., $\sim$4.1 eV below the bottom of the conduction band of LGO (see Fig. 6).

The above results demonstrate the possibility of very large ($\sim$eV) relative shifts of the positions in the host energy gap of the levels of the same impurity ion located at different types of complex centers, differing in the nature of the position of the nearby charge-compensating defect. This situation is observable when the impurity site lacks inversion symmetry leading to a permanent dipole moment. The large relative shift of the levels is due to the strong linear Stark shift of electronic states of the ion in the Coulomb field of a nearby charged defect. In the case of Cr^{3+} in the LGO lattice, the electric Coulomb field generated by $Mg^{2+}(2)$ at the Cr^{3+} is on the order of 10^7 V/cm.[2] With the observed value of the linear Stark shift of 0.6 eV one can estimate the magnitude of the permanent dipole of the Cr^{3+} ion to be $\sim$1 D.

VII. CONCLUSION

The results for LGO:Cr described here demonstrate the importance of considering both donorlike and *acceptorlike* processes, i.e., treating the host-impurity system as an entirety, for hole burning in doped insulators. This is most important when the host band gap is not too wide compared to the energies of the intra-ion transitions constituting the first step for the hole burning. Using a combination of absorption, excitation, and photoexcitation spectroscopy, the energy locations of the $^4A_2$ and ^2E energy levels with respect to the host bands for three different charge-compensated Cr^{3+} centers were determined. For the Cr^{3+}-Mg(2) site that undergoes hole burning, the *R*-line photon is sufficiently energetic to promote an electron from the ^2E excited state to the conduction band, but lacks the energy to induce acceptorlike transitions which would erase the hole. For the Cr^{3+}-Li site, photoionization is possible, but acceptorlike transitions can also occur, efficiently competing with the photoionization preventing the occurrence of a stable hole. For the Cr^{3+}-Mg(1) center, the *R*-line photon energy is insufficient to produce photoionization from the ^2E excited state. These large differences in the energy locations of the Cr^{3+} levels in the host band gap, as much as 10% of the band-gap energy, are caused by the absence of inversion symmetry at all three sites, which results in large linear Stark effects of about 1 eV.

ACKNOWLEDGMENTS

This work was supported in part by the National Science Foundation, Grant Nos. DMR-9307610 and DMR-9321052, and by the Russian Foundation of Basic Research, Grant No. RFBR 99-02-18319.

*Present address: Changwon National University, Korea.

[1] R. M. Macfarlane and R. M. Shelby, in *Persistent Spectral Hole Burning: Science and Applications*, edited by W. E. Moerner (Springer-Verlag, Berlin, 1988), p. 127.

[2] S. A. Basun, A. A. Kaplyanskii, and S. P. Feofilov, Phys. Solid State **36**, 1821 (1994), and references therein.

[3] M. Wada and Y. Ishibashi, J. Phys. Soc. Jpn. **52**, 193 (1983).

[4] Y. Iwata, I. Shibuya, M. Wada, A. Sawata, and Y. Ishibashi, J. Phys. Soc. Jpn. **56**, 2420 (1987).

[5] S. A. Basun, S. P. Feofilov, and A. A. Kaplyanskii, Ferroelectrics **143**, 163 (1993).

[6] G. F. Imbusch and W. M. Yen, *Ruby—Solid State Spectroscopy's Serendipitous Servant*, in *Lasers, Spectroscopy and New Ideas*, edited by W. M. Yen and M. D. Levenson (Springer-Verlag, Berlin, 1987).

[7] S. Majetich, D. Boye, J. E. Rives, and R. S. Meltzer, J. Lumin. **40/41**, 307 (1988).

[8] R. Wannemacher and R. S. Meltzer, J. Lumin. **43**, 251 (1989).

[9] M. Born, Verh. Dtsch. Phys. Ges. **21**, 679 (1919); F. Haber, *ibid.* **21**, 750 (1919).

[10] B. Sevastyanov and M. Sharonov (private communication). The estimation of E_g was made on the basis of the spectral location of the fundamental absorption edge of LGO.

[11] S. A. Basun, U. Bianchi, V. E. Bursian, A. A. Kaplyanskii, W. Kleeman, L. S. Sochava, and V. S. Vikhnin, J. Lumin. **66/67**, 526 (1995).

[12] A. J. Silversmith, W. Lenth, K. W. Blazey, and R. M. Macfarlane, J. Lumin. **59**, 269 (1994).